International Journal of Scientific Engineering and Technology
Volume No.5 Issue No.6, pp: 326-330

ISSN:2277-1581
01 June 2016

Preparation of $La_{0.9}Sr_{0.1}MnO_{3-\delta}$ (LSM) Thin Films by Spray Pyrolysis Technique for SOFC Cathode

[1]B. S. Kamble, [2]V. J. Fulari, [3]R. K. Nimat*

[1]Department of Physics, D.B.J.College, Chiplun-415605, India
[2]Department of Physics, Shivaji University, Kolhapur-416004, India
[3]Department of Physics, Balasaheb Desai College, Patan-415206, India
E-mail:- dr_rknimat@yahoo.com

Abstract:Strontium-doped lanthanum manganite ($La_{0.9}Sr_{0.1}MnO_{3-\delta}$) were synthesized by spray pyrolysis technique in the thin film form on alumina substrate. The $La_{0.9}Sr_{0.1}MnO_{3-\delta}$ (LSM) thin films were sintered in the step of 150 ^oC from 600^oC to 900^oC. X-ray diffraction study confirmed phase formation of LSM and Infrared spectroscopy confirmed perovskite structure. Morphology of LSM has been studied by using Scanning electron microscopy and Atomic force microscopy, shown porosity within homogeneous grain structure. TGA/DSC and DTA study exhibits stable crystallization after 700^oC. Dielectric study shows mixed electrical conduction at the grain boundary interface in the sample.

Keywords: *Spray Pyrolysis, Cathode, LSM, SOFC.*

Introduction:

The Solid Oxide Fuel Cell (SOFC) is a device which directly converts chemical to electrical energy [1]. When compared with conventional methods of power generation, SOFCs have many advantages such as high energy conversion, easy modular construction [2]. The most SOFCs are operated at high temperatures up to 600^{o}C-1000^{o}C and are based electrolyte used [3,4]. The Lanthanum Strontium Manganite (LSM) is good material as cathode for SOFC [5,6]. A solid oxide fuel cell is a device that converts the chemical energy of fuels directly into electrical energy by an electrochemical reaction of the fuels with an oxidant. Lanthanum strontium manganite ($La_{1-x}Sr_xMnO_3$-LSM) is mostly used as a cathode for SOFC as it is highly electrochemically active for oxygen reduction. The LSM is thermally and chemically stable and compatibility with yittri stabilized zerconia (YSZ) electrolyte [7, 8]. A perovskite with general formula ABO_3, where 'A' stands for 'La' or 'Sr' and 'B' stands for 'Mn' in case of LSM shown in fig. 1 [9].

The use of LSM cathode in bulk form is not applicable for a low-temperature SOFC, due to its low oxygen ion conductivity and high activation energy [10]. The attempts made that to form LSM thin film as possibly to reduce the operating temperature [11]. The LSM thin films which are used as cathode for SOFC are synthesized by Chemical Spray pyrolysis. The Spray pyrolysis is the cheap and effective technique due to possibly adherent thin films.

In this study, we report the preparation of strontium doped lanthanum manganite with a composition $La_{0.9}Sr_{0.1}MnO_{3-\delta}$ (LSM) by the cost effective spray pyrolysis technique and are characterized by TGA/DSC, XRD, SEM, AFM and IR spectroscopy.

Experimental:

The Lanthanum Strontium Manganite ($La_{1-x}Sr_xMnO_{3-\delta}$) thin films were deposited on alumina substrate by using Chemical Spray Pyrolysis technique. The basic principle used in chemical spray pyrolysis technique is that, a smallest droplet of the precursor solution sprayed from nozzle, reaches to the hot substrate leads to the pyrolytic decomposition of the solution which forms the adherent thin films in the presence of air as neutral gas [12].

The appropriate amount of precursor were dissolved into double distilled water in to constant stirring in order to maintain the stoichiometry of final product which deposit on alumina (Al_2O_3) substrate at 250^{o}C, this further leads to pyrolytic decomposition of these metallic salts [13] and formation of Lanthanum Strontium Manganite thin film. The precursor flow rate is maintained 3 ml/min, the nozzle to substrate distance is 20 cm and adherent thin films were obtained. The post deposition annealing conditions were chosen to be 2 hours at 600^{o}C, 750^{o}C and 900^{o}C in air. The deposited $La_{0.9}Sr_{0.1}MnO_3$ (LSM) thin film was used for structural and spectroscopic characterization. The flow chart of spray system are shown in Fig.1.The phase of LSM was checked by X-ray diffraction (Brucker X-Ray Powder diffractometer cu kα radiation) and the morphology was probed by Jeol Scanning Electron Microscope (SEM). TGA/DSC was carried out by SDT Q600 V20.9 Build 20 instrument in nitrogen at 10^{o}C/min.

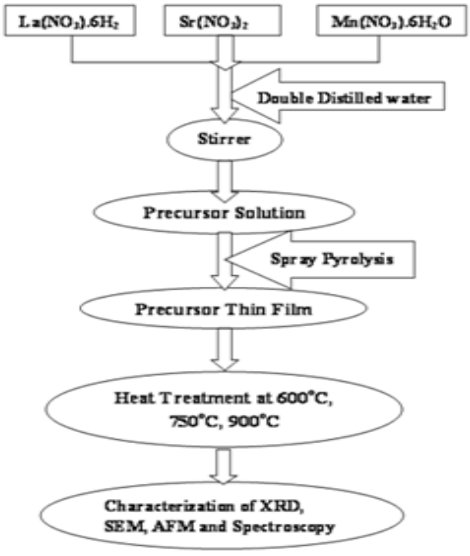

Fig. 1. Flow Chart of Spray System

International Journal of Scientific Engineering and Technology
Volume No.5 Issue No.6, pp: 326-330
ISSN:2277-1581
01 June 2016

Result and Discussion:

A) Thermal Characterization:

The TGA/DSC and DTA curves are shown in fig. 2a) and fig. 2b) respectively. For the LSM thin film the thermal decomposition process occurs in the four steps between 30°C to 1000°C and the total weight loss is 1.760 mg. The first step of thermal decomposition between 30°C to 100°C is related to the mass loss of water. The gas absorbed on the surface of substrate and polymer degradation occurs in the second step up to 300°C. In the third step between 300°C to 650°C the mass loss is due to decomposition of metal salts and phase formation started. Finally the material begins to stabilize at 750°C (fourth step). The first weight loss of 0.3713 mg, could be attributed to evaporation of water. The second weight losses of 0.5131 mg, corresponds to decomposition of nitrates.

The third weight loss of 0.8165 mg is due to evaporation of water. The highest decomposition temperature at about 750°C is due to presence of strontium nitrates. The DTA curve shows the exothermic peaks at 100°C, near to 600°C and at 900°C, this corresponds to mass loss of water observed in TGA curve. Both TGA and DTA curve shows the stable crystallization of $La_{0.1}Sr_{0.9}MnO_{3-\delta}$ (LSM) after 700°C.

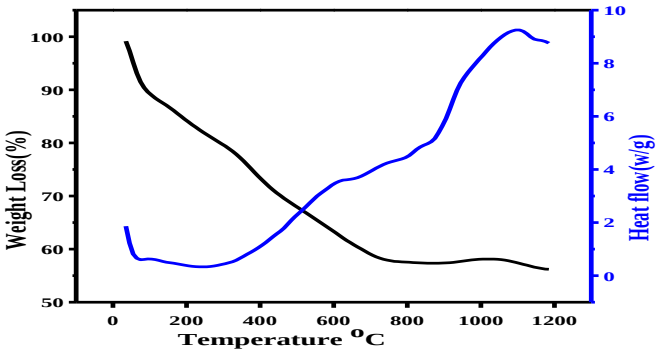

Fig. 2a) The TGA/DSC curve of LSM

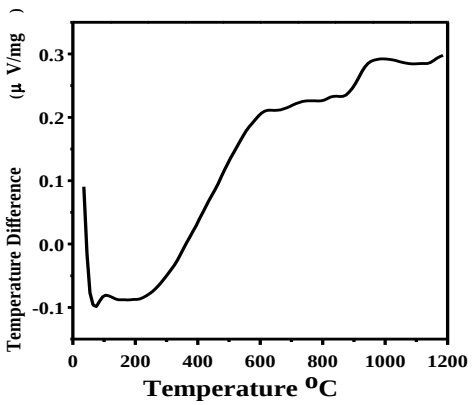

Fig. 2b) The DTA curve of LSM

B) Structural Characterization:

The XRD patterns of LSM thin films deposited at substrate temperature 250°C and sintered in air for 2 hours at 600, 750°C and 900°C are shown in fig. 3. The XRD analysis was done by JCPDS file nos. 047-0444 ($La_{0.9}Sr_{0.1}MnO_3$) and 83-2080 (Al_2O_3). The substrate peaks were observed due to low thickness of film. The observed lattice parameters are a=b=5.5336 Å, c=13.3560 Å, α=β=90°, γ=120° and wavelength of X-ray used for analysis was λ=1.5418 Å. The XRD study confirms trigonal crystal structure with space group $R\bar{3}c$. The unit cell is rhombohedral with hexagonal lattice parameter. The XRD study shows maximum intense peaks for sintering temperature 900°C. The peak of maximum intensity shows the

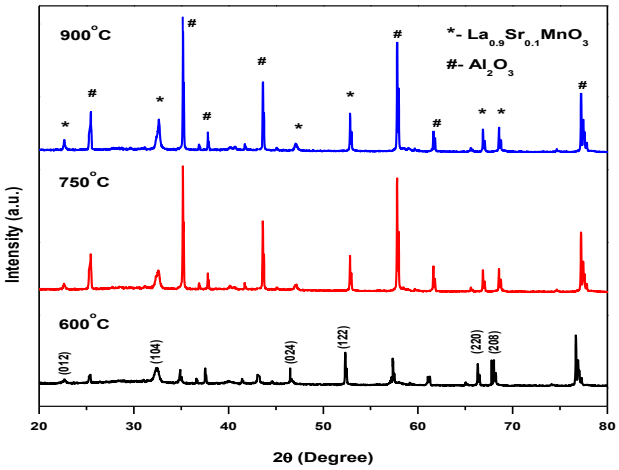

average crystallite size is about 38 nm, calculated by Scherrer equation, $D = \frac{K\lambda}{\beta \cos\theta}$ [14].

Fig.3) The XRD of LSM

C) Morphological Characterization:

The morphological study of LSM thin film was made by JEOL Scanning Electron Microscope. The SEM images show porous morphology which represents its suitability as cathode for solid oxide fuel cell and it is necessary in order to pass oxygen ions at cathode- electrolyte interface [15]. The porosity provides maximum surface area leads to more reaction sites for oxygen reduction in fuel cell cathodes [16]. The morphology of $La_{0.9}Sr_{0.1}MnO_{3-\delta}$ thin films sintered at 600°C, 750°C, 900°C shown in Fig. 4, 5 and 6 respectively. The SEM micrograph shows the improvement of size homogeneity of the samples [15].

The AFM micrograph illustrates the granular structure for deposited thin films. (Fig.7,8 and Fig.9). Root mean square (rms) roughness of LSM thin film were estimated to be 45.3 nm, 31.3nm and 38.6 nm for T = 600°C, T=750°C and T = 900°C respectively. A homogenous grain structure can be seen with no second phase [17]

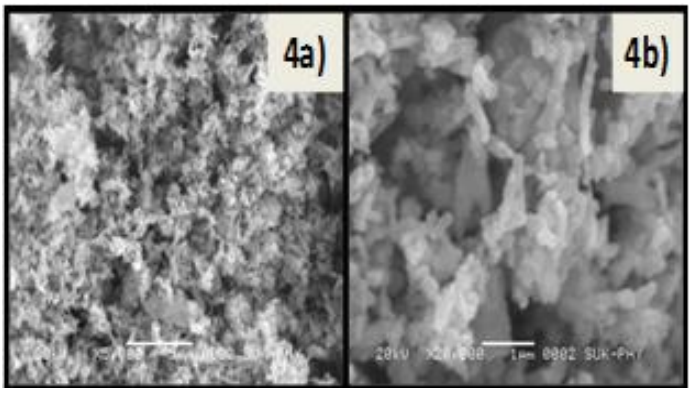

International Journal of Scientific Engineering and Technology
Volume No.5 Issue No.6, pp: 326-330
ISSN:2277-1581
01 June 2016

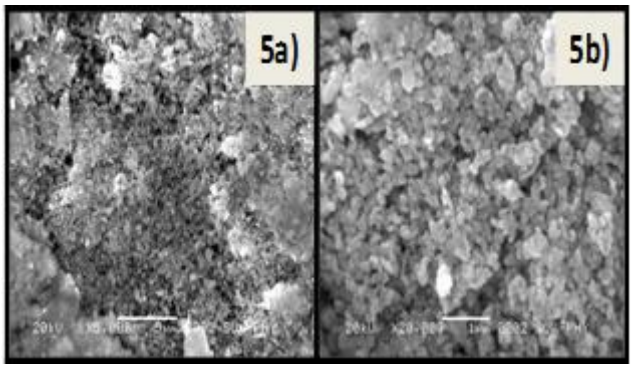

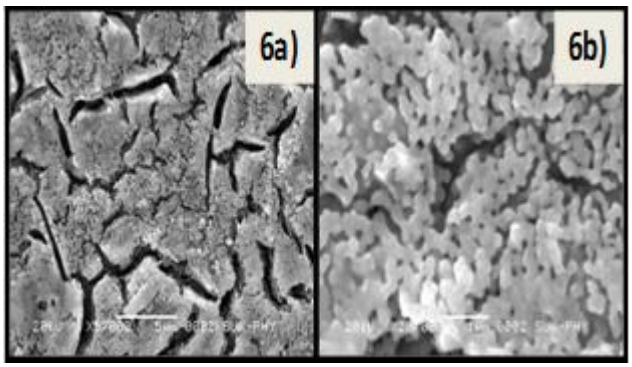

Fig.4,5,6 The SEM images of LSM thin films sintered at 600, 750 and 900^{o}C respectively.

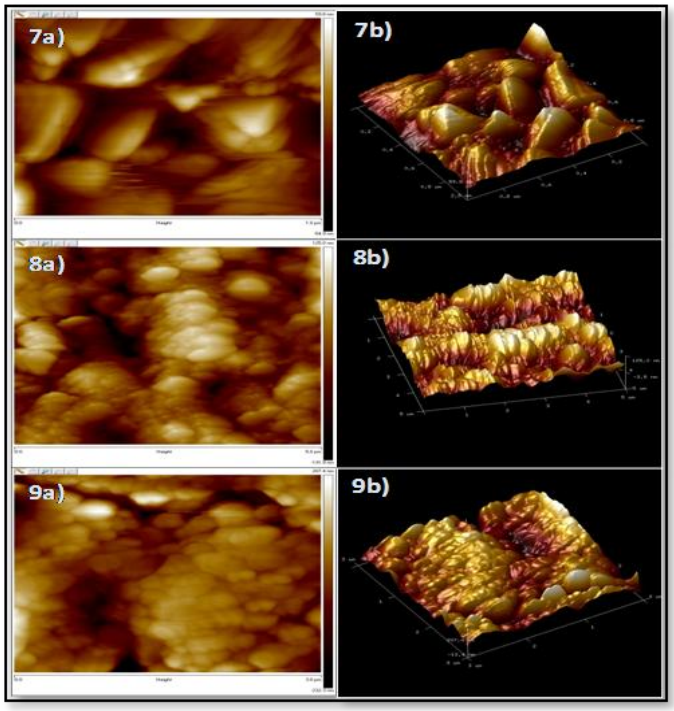

Fig.7 a),8 a),9a) are 2-D and 7 b), 8 b), 9b) are 3-D AFM images of LSM Sintered at 600, 750, 900^{o}C respectively.

D) Spectroscopic Characterization:

The IR transmission spectra of strontium doped lanthanum manganite were prepared by spray pyrolysis technique are shown figure 10(a) represents IR absorption of as prepared sample while fig.10(b), 10(c) and 10(d) represents the chemistry for the formation of LSM perovskite materials with variations in sintering temperatures from 600 to 900^{o}C in the step of 150 ^{o}C by the help of IR absorption. A broad peak at 3450.94 cm^{-1} in asprepared sample due to stretching mode of hydroxyl group of bond water molecules, which gradually minimizes when sintering at 600^{o}C. The broad peak around 2923.54 cm $^{-1}$ is due to asymmetric stretching of CH_2 group. In asprepared sample strong absorption peak at 755cm^{-1} and 1359cm^{-1} are due to nitrates which were diminishes with sintering. Additionally, in sintering LSM samples with absorption band at 1459.39cm^{-1} are due to C=O vibration and can be related to traces of carbonate. Figure10.also shows a clean IR spectrum with an absorption peak at 618.10cm^{-1} corresponding to the stretching mode which involves the internal motion of change in Mn-O-Mn bond length. This represents the formation of crystalline powder containing the LSM perovskite structure material which is in agreement with the result of XRD [8].

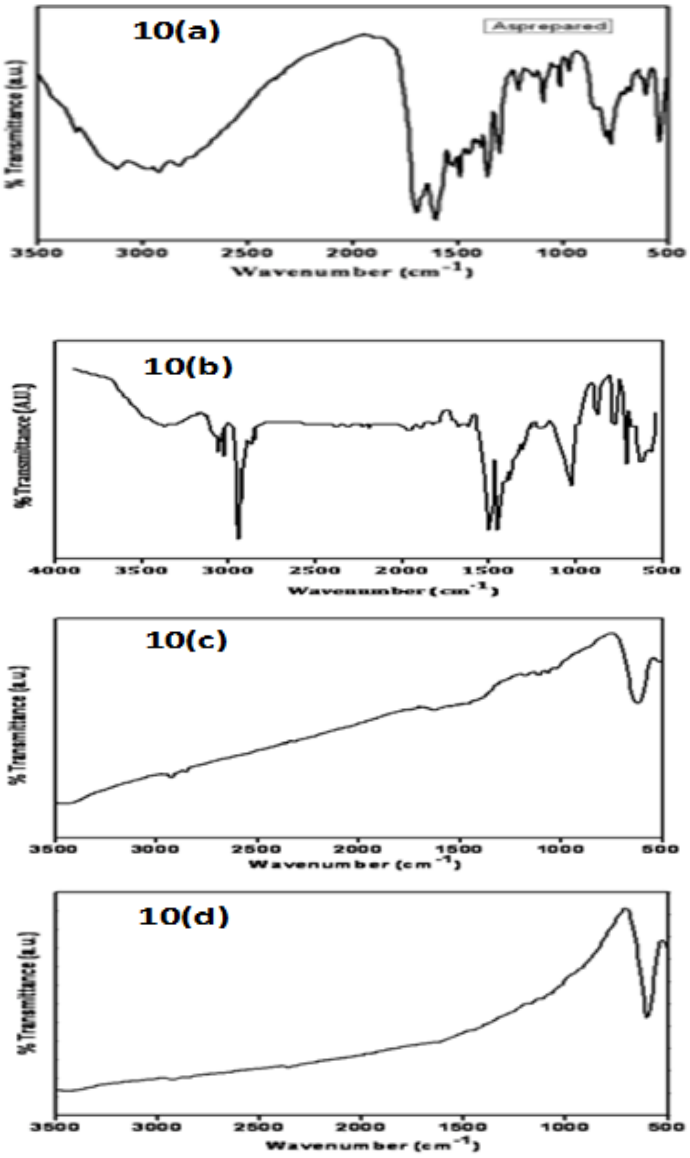

Fig.10 (a, b, c and d) IR absorption pattern of LSM sintered at asprepared sample, 600,750 and 900^{o}C respectively.

ISSN:2277-1581
01 June 2016

3.5.1 Dielectric study:

The Fig.11 Gives the plot of dielectric constant vs. frequency of LSM thin film sintered at 600°C,750°C and 900°C. The dielectric constant of LSM decreases with the increase in frequency within the frequency range (0-1 MHz). The dielectric constant of material is due to the ionic, electronic, dipolar and surface charge polarizations which depend on the frequencies. The dielectric constant have larger values at lower frequency, it may be due to the space charge polarization arising at the grain boundary interfaces [18]. The low frequency dielectric relaxation is due to space charge polarization arises at grain boundary interface which predicts different electrical conductivities at contact due to hopping mechanism within localized charge carriers in LSM thin film [19, 20].

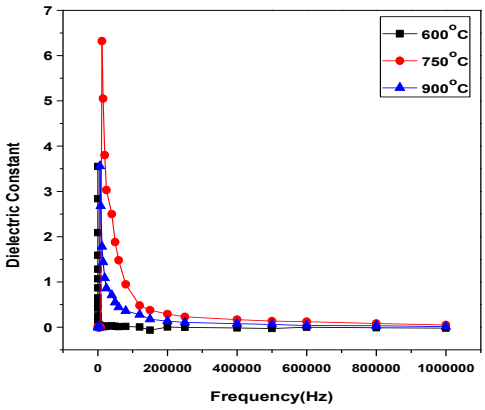

Fig.11 Dielectric Constant Vs Frequency

Conclusion:

The $La_{0.9}Sr_{0.1}MnO_{3-\delta}$ (LSM) thin films were successfully synthesized by Spray Pyrolysis technique. XRD pattern of LSM exhibits trigonal crystal structure with space group $R\bar{3}c$. The average crystallite size was found to be 38 nm from maximum intense peak. As sintering temperature of LSM thin films increases, the SEM micrographs show the improvement of homogeneity with porosity. AFM micrographs show that homogenous grain structure. IR spectrum reveals the formation of LSM perovskite structure. The dielectric dispersion with increase in frequency shows good prediction of heterogeneous or mixed electrical conduction at contact. The heterogeneous or mixed conduction with porosity in $La_{0.9}Sr_{0.1}MnO_{3-\delta}$ (LSM) thin film reveals its applicability as SOFC cathode.

References:

i. *H. A. Hamedani, K. H. Dahmen, D. Li, H. Peydaye-saheli, H. Garmestani, M. Khaleel. Materials Science and eingineering B, 153 (2008), 1-9.*

ii. *J. C. Marrero, N. F. Ribero, C. F. Malfatti, M. M. Souza, Journal of Advanced Ceramics 2 (2013) 55-62.*

iii. *M. R. Cesario, D. A.Macedo, R. M. P. B. Oliveria, P. M. Pimental, R. L. Moreira and D. M. A. Melo, Journal of Ceramic Processing Research 12 (2011) 102-105.*

iv. *A. J. Jacobson, Chemistry materials 22 (2010) 660-674.*

v. *V. Channu, R. Holze, E. Walker, New Journal of Glass and Ceramics 3 (2013) 29-33.*

vi. *E. Quennevile, M. Meunier and A. Yelon, Journal of Applied Physics,90, No. 4 (2001).*

vii. *M. Gupta, P. Yadav, W. Khan, A. Azam, A. h. Naqvi, R.K. Kotnala, Advanced material letters (2012) 3 220-225.*

viii. *H. B. Wang, G. Y. Meng, D. K. Peng, Thin solid Films 368(2000), 275-278.*

ix. *J. Richter, P. Holtappels, T. Graule, T. Nakamura, L. J. Gauckler, Monatsh Chem 140 (2009) 985-999.*

x. *K. Gupta, P. C. Jana, A. K. Meikap and T. K. Nath, Journal of Applied Physics 107 (2010) 073704-073704.*

xi. *R. K. Nimat, R. S. Joshi, S. H. Pawar, Journal of Alloys and Compound 466 (2008) 341-351.*

xii. *R. Chiba, R. A. Vargas, M. Andreoli, E. S. M. Seo, Materials Science Forum 591 (2008) 459-464*

xiii. *S. Calderon V, L. Escobar-Alarcon, E. Vamps, S.Muhl, M. Rivera, I. Bentacourt, J. Olaya, A. Marono, Microelectronics Journal 39 (2008) 1281-1283.*

xiv. *D. Grossin, J. G. Noudem, Solid State Sciences 6 (2004) 939-944..*

xv. *D. W. Kim, D. H. Kim, T. W. Noh, E. Oh, H. C. Kim, H. C. Lee, Solid State Communications 121 (2002) 631- 634.*

xvi. *X. Ding, C. Cui, X. Du, L. Guo, Journal of Alloys and Compounds 475 (2009) 418-421.*

xvii. *H. S. Al-Jumaili, A. S. Mohammed, International Journal of Emerging Technology and Advanced Engineering 3 (2013) 39-43.*

xviii. *S. Devikala, P. Kamaraj, M. Arthanareeswari, Chemical Science Transactions 2 (2013) 129-134.*

xix. *X. S. Fang, C. H. Ye, T. Xie, Z. Y. Wong, J. W. Zhao and L. D. Zhang, Applied Physics Letters 88 (2006) 013101-013103.*

xx. *L. Singh, U. S. Rai, K. D. Mandal, Advances in Applied Ceramics 111 (2012) 374-380.*